International Journal of Applied Earth Observations and Geoinformation 107 (2022) 102697

Contents lists available at ScienceDirect

International Journal of Applied Earth Observations and Geoinformation

journal homepage: www.elsevier.com/locate/jag

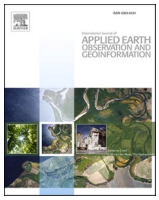

Farming and Earth Observation: Sentinel-2 data to estimate within-field wheat grain yield

Joel Segarra [a,b], Jose Luis Araus [a,b,*], Shawn C. Kefauver [a,b,*]

[a] Integrative Crop Ecophysiology Group, Plant Physiology Section, Faculty of Biology, University of Barcelona, 08028 Barcelona, Catalonia, Spain
[b] AGROTECNIO (Center for Research in Agrotechnology), Av. Rovira Roure 191, 25198 Lleida, Catalonia, Spain

ARTICLE INFO

Keywords:
Grain yield
Machine learning
Precision farming
Remote sensing
Sentinel-2
Wheat

ABSTRACT

Wheat grain yield (GY) is a crop feature of central importance affecting agricultural, environmental, and socioeconomic sustainability worldwide. Hence, the estimation of within-field variability of GY is pivotal for the agricultural management, especially in the current global change context. In this sense, Earth Observation Systems (EOS) are key technologies that use satellite data to monitor crop yield, which can guide the application of precision farming. Yet, novel research is required to improve the multiplatform integration of data, including data processing, and the application of this discipline in agricultural management. This article provides a novel methodological analysis and assessment of its applications in precision farming. It presents an integration of wheat GY, Global Positioning Systems (GPS), combine harvester data, and EOS Sentinel-2 multispectral bands. Moreover, it compares several indices and machine learning (ML) approaches to map within-field wheat GY. It also analyses the importance of multi-date remote sensing imagery and explores its potential applications in precision agriculture. The study was conducted in Spain, a major European wheat producer. Within-field GY data was obtained from a GPS combine harvester machine for 8 fields over three seasons (2017–2019) and consecutively processed to match Sentinel-2 10 m pixel size. Seven vegetation indices (NDVI, GNDVI, EVI, RVI, TGI, CVI and NGRDI) as well as the biophysical parameter LAI (leaf area index) retrieved with radiative transfer models (RTM) were calculated from Sentinel-2 bands. Sentinel-2 10 m resolution bands alone were also used as variables. Random forest, support vector machine and boosted regressions were used as modelling approaches, and multilinear regression was calculated as baseline. Different combinations of dates of measurement were tested to find the most suitable model feeding data. LAI retrieved from RTM had a slightly improved performance in estimating within-field GY in comparison with vegetation indices or Sentinel-2 bands alone. At validation, the use of multi-date Sentinel-2 data was found to be the most suitable in comparison with single date images. Thus, the model developed with random forest regression (e.g. $R^2 = 0.89$, and RSME = 0.74 t/ha when using LAI) outperformed support vector machine ($R^2 = 0.84$ and RSME = 0.92 t/ha), boosting regression ($R^2 = 0.85$ and RSME = 0.88 t/ha) and multilinear regression ($R^2 = 0.69$ and RSME = 1.29 t/ha). However, single date images at specific phenological stages (e.g. $R^2 = 0.84$, and RSME = 0.88 t/ha using random forest at stem elongation) also posed relatively high R^2 and low RMSE, with potential for precision farming management before harvest.

1. Introduction

Crop yield gathers maximum attention in agricultural research and public policies due to its importance for guiding economic decisions and ensuring farmers' incomes and food security (Rosegrant and Cline, 2003; van Ittersum, 2016). In the current global context, crop management faces several challenges which affect negatively both the production and the environment. On the one hand, crop yield is highly dependent on external inputs (Sutton et al., 2011), which, when mismanaged, can lead to environmental pollution and a decline in the performance. On the other hand, crop yields are highly susceptible to external pressures such as climatic conditions or pests (Savary et al., 2019), as well as of spatial variability in soil fertility which jeopardize the performance of crops. Therefore, the high-resolution prediction of crop yields before harvest plays a central role in addressing these challenges and guiding management decisions affecting agricultural,

* Corresponding authors at: Integrative Crop Ecophysiology Group, Plant Physiology Section, Faculty of Biology, University of Barcelona, 08028 Barcelona, Catalonia, Spain.
E-mail addresses: jaraus@ub.edu (J.L. Araus), sckefauver@ub.edu (S.C. Kefauver).

https://doi.org/10.1016/j.jag.2022.102697
Received 25 October 2021; Received in revised form 21 January 2022; Accepted 23 January 2022
Available online 5 February 2022

environmental, and socioeconomic sustainability. In this sense, Earth Observation Systems (EOS) are key technologies that use satellite data and can be used to monitor crop yield and potentially guide the application of management strategies within precision agriculture. In the last years, EOS have improved their resolutions and consequently the potential to apply precision agriculture in crop management has increased (Migdall et al., 2018), as well as the capacities to monitor environmental features affecting crops (Hunt et al., 2019b).

Among the current openly accessible EOS, the system that has gathered more attention in recent years in precision agriculture is Sentinel-2. Since its full operationality was reached in 2018, the European-launched satellite has a revisit time of 5 days, in addition to an improved spatial and spectral resolution in comparison with other equivalent satellites (Segarra et al., 2020a) used in precision farming. The open access nature of Sentinel-2 data is also a central factor for its use, as many high to middle resolution satellites have paywalls. In addition to EOS, other technological advancements such as Global Positioning System (GPS)-supported agricultural machinery have been developed in the last years and allows for a multiplatform development of precision agriculture (Bach and Mauser, 2018). These technological advancements can coordinate to monitor key agricultural features such as yield in a more efficient fashion. Besides the technological advancements, modelling approaches such as machine learning (ML) have shown considerable promise in agricultural remote sensing applications (Chlingaryan et al., 2018). These ML computer algorithms are particularly useful for studying complex biological systems, as they can capture complex interactions among variables and find generalizable predictive patterns (Bzdok et al., 2018). The use of multiplatform data to develop models that allow estimating grain yield before harvest is central to guiding agricultural management and both secure crop yield and optimize the use of resources (Foley et al., 2011).

Sentinel-2 data in combination with GPS combine harvesters can contribute to precisely generate grain yield (GY) estimation models. Nonetheless, the potential for estimating within-field GY variability has yet to be fully explored and calls for a further integration of multiplatform data and streamline data processing. In the case of Sentinel-2, only a few articles have dealt with remote sensing and GPS combine harvesters, as for example the case of cereals maize (Kayad et al., 2019) and wheat (Cavalaris et al., 2021; Hunt et al., 2019b). For maize, ML random forest (RF) and support vector machine (SVM) regressions were tested to match Sentinel-2 vegetation indices with GPS GY points at a single field. The results were modest ($R^2 = 0.48$) but showed potential in determining the best phenological stage when estimating within-field GY. In the case of wheat, Cavalaris et al. (2021) demonstrated the possibility to match Sentinel-2 derived vegetation indices (VIs) with within-field GY using simple regressions at different phenological stages ($R^2 = 0.63$). Also in wheat, Hunt et al. (2019) used RF, VIs and Sentinel-2 bands alone to estimate wheat within-field GY in a single season. Their results suggested that Sentinel-2 bands alone and VIs have similar results ($R^2 = 0.89$).

So far, however, biophysical variables, such as LAI (leaf area index), derived from radiative transfer models (RTM) have not been used in estimating within-field wheat GY. Overall, VIs have limitations in the radiometric information they can exploit and are not as robust as RTM (Maes and Steppe, 2019; Weiss et al., 2000). In this sense, and compared with VIs, LAI has shown improvements for grain yield estimation for several crops (Duan et al., 2021; Gilardelli et al., 2019; Lambert et al., 2018; Mokhtari et al., 2018; Zhou et al., 2017). Moreover, in the case of wheat, so far ML approaches have not been matched with phenological stages, which could be relevant to precision agriculture management needs for crop-specific models. Furthermore, in the case of wheat within-field grain yield, ML learning approaches have not been fully explored, as only simple regressions and RF have been tested. In this sense, support vector machine (SVM) was also tested for within-field maize grain yield estimation (Kayad et al., 2019), but the study focused exclusively on the use of vegetation indices. Similarly, boosted regression (BR) has shown improved performance for yield estimation applied to winter wheat compared to SVM by several authors (Heremans et al., 2015; Stas et al., 2016), but again both studies used only vegetation indices and lower-resolution satellite data.

We aim to make the most of current technological advancements to define the most suitable variables for estimating within-field wheat GY. On the one hand, we use GPS technological advancements in combine harvesters, which have provided large (within fields) geolocated grain yield datasets. On the other hand, we match this data with remotely sensed Sentinel-2 satellite spectral information and RTM to feed ML GY estimation models. Over three seasons (2017–2019) eight different fields in the Province of Burgos (Spain) were monitored with Sentinel-2 time series, biophysical parameter LAI derived from RTM and different VIs (NDVI, GNDVI, EVI,. RVI, TGI, CVI and NGRDI) were calculated for each field over the various image dates obtained throughout the seasons. The Sentinel-2 bands alone, the biophysical parameter and VIs were independently matched to the GPS combine harvester dataset. The ML approaches RF, SVM, generalized boosting regression (BR), together with a multilinear regression as baseline, were used. The study was structured around three questions.

1) What processing or combination of Sentinel-2 derived spectral information is more suitable to estimate within-field wheat grain yield?
2) Can wheat GY models matching phenological stages be accurate and have potential to be applied in precision agriculture?
3) Which ML approach is more suitable for high resolution crop-specific wheat grain yield modelling?

This study concludes by discussing the potential of the findings presented here to be applied in field-level management for precision farming. Moreover, it suggests some guidelines to advance towards a generalized use of these technologies among farmers.

2. Materials and methods

2.1. Study site

The study was conducted during three seasons (2017–2019) in the Province of Burgos. The region where this study takes place is the Northern inner plateaus (*Meseta Norte*) of Spain. This region is in the Duero Basin and is characterized by agricultural fields growing mainly winter cereals (barley and wheat). Regarding wheat types, Spain is among the top durum wheat producers in Europe (Ranieri, 2015), with the Duero Basin region (Castilla y León) being among the largest producers at the country level after Andalucía in Southern Spain. Data from 8 fields in the Province of Burgos in Spain (Fig. 1) were used. Fields were conventionally managed and the variety Athoris of durum wheat (*Triticum turgidum* L. subsp. *durum* (Desf) Husn.), which is widely grown in the region, was sowed. The location of the fields is shown in Fig. 2.

Meseta Norte has an inner-Mediterranean/continental climate with an average temperature of 10–14 °C, annual rainfall under 600 mm and average height above sea level of 800–850 m (Font Tullot, 2000). The fields were sown between mid-October and first week of November for the three seasons. The fields were fertilized with chemical fertilizers averaging between 35 and 40 kg/ha of N, 80–130 kg/ha of P and 60–90 kg/ha of K in the case of basal fertilization. Regarding top-dressing fertilization, between 85 and 110 kg/ha N was applied throughout the three seasons in the different fields between tillering and stem elongation, corresponding to Z30-Z32 phenological stages (Zadoks et al., 1974). The average grain yield over the three seasons was 4.81 t/ha.

Regarding the description of the fields shown in Fig. 2, number 1 has a surface of 21.30 ha and a slope of less than 1%, number 2 has a surface of 25.80 ha and a slope of less than 1%, number 3 has a surface of 5.80 ha and a slope of 3%, number 4 has surface of 55.64 and a slope of 7%, number 5 has a surface of 18.50 ha and a slope of 2%, and number 6 has

Fig. 1. Map of the Iberian Peninsula with the province of Burgos, where the fields are located, highlighted in green. (For interpretation of the references to color in this figure legend, the reader is referred to the web version of this article.)

a surface of 9.70 ha and a slope of 2%. The area is characterized by loam/clay soils with a homogenous distribution (https://suelos.itacyl.es/mapas).

2.2. Sentinel-2 data and indices calculation

The Sentinel-2 multispectral bands (Table. 1) were downloaded without cloud cover from Copernicus Open Access Hub (https://scihub.copernicus.eu/) as a 2A product (Bottom of Atmosphere reflectance images) for the following dates: 2017 (05–22), 2018 (04–17, 05–26), 2019 (04–12, 05–12). In addition, the imagery captured on 04–14-2017 was downloaded as a L1C product (Top of Atmosphere reflectance images) and was subsequently corrected to level 2A using the Sen2Cor tool on SNAP (Sentinel Application Platform), obtaining Bottom-Of-Atmosphere (BOA) and cirrus corrected reflectance images. The sensing dates were matched to the phenological stages in situ evaluated following the Zadoks scale (Zadoks et al., 1974): stem elongation (30–39), heading (41–59) and anthesis (61–69).

Seven widely used VIs (Table 2) were calculated on ArcGIS Pro 2.3.0 as shown in Table 2. Moreover, the biophysical parameter, LAI (leaf area index) was calculated at 10 m of spatial resolution following neural network algorithms trained with PROSAIL radiative transfer models (Weiss and Baret, 2016) on SNAP (Sentinel Application Platform) (Table. 2).

2.3. Matching of sentinel-2 and GPS combine harvester grain yield data

The fields were harvested between mid-July to the beginning of August throughout the three seasons. A combine harvester (John Deere T660i + 625R) equipped with a GPS was used and relative GY results (t/ha) were reported. As the obtained results were relative to the surface and not absolute weights, we considered that no calibration between actual weight and harvested weight was necessary. All GPS GY points obtained with the combine harvester were uploaded as a shapefile in ArcGIS Pro 2.3.0, and subsequently all points contained within each pixel were averaged using the Spatial Analysis Menu Tool Point to Raster. As a result, each single pixel value of the calculated LAI, NDVI, GNDVI, EVI, RVI, TGI, CVI and NGRDI layers and the original 10 m resolution Sentinel-2 bands were associated to one GY value. This processing protocol was carried out at each phenological stage. An overview of few indices calculated is shown in Fig. 3. A total number of 20,124 pixels with their corresponding unique GY values and Sentinel-2 derived data was obtained as data set. The raw data was manually buffered to avoid edge effects of mix pixels as shown in Fig. 4. All the data was matched in a point vector file, it was easier to process and use as data is organized in attribute tables. The processing was carried out on ArcGIS Pro 2.3.0 and a schematic illustration describing the process is shown in Fig. 4. The cut width of the combine harvester was 7.60 m and therefore adequate to 10 m pixels size of Sentinel-2 imagery. Notwithstanding its suitability for Sentinel-2 pixel size, the GY spatial resolution of the combine harvester, as it is a function of the monitoring equipment, the cutting head and the software has some lack of precision, as reported by other authors (Lyle et al., 2014).

All the GPS GY points with values lower to 0.5 t/ha were discarded. Moreover, a portion of the raw data was trimmed using the “tclust” package in R (R Core Team, 2021) based on GY and Sentinel-2 bands inaccuracies. Trimming allows the removal of the most outlying data which can strongly influence the results; this approach has been introduced by several authors (García-Escudero et al., 2008; Woodruff and Reiners, 2004). The number of clusters (k) and portion of data trimmed (α) was optimized and subsequently applied to remove outliers ($k = 5$, $\alpha = 0.05$). The general process is sh own in Fig. 5.

2.4. Machine learning approaches

One of the most widely used machine learning (ML) approaches is random forest (RF) regression. It has been successfully used for estimating wheat grain yield (Hunt et al., 2019a; Jeong et al., 2016; Wang

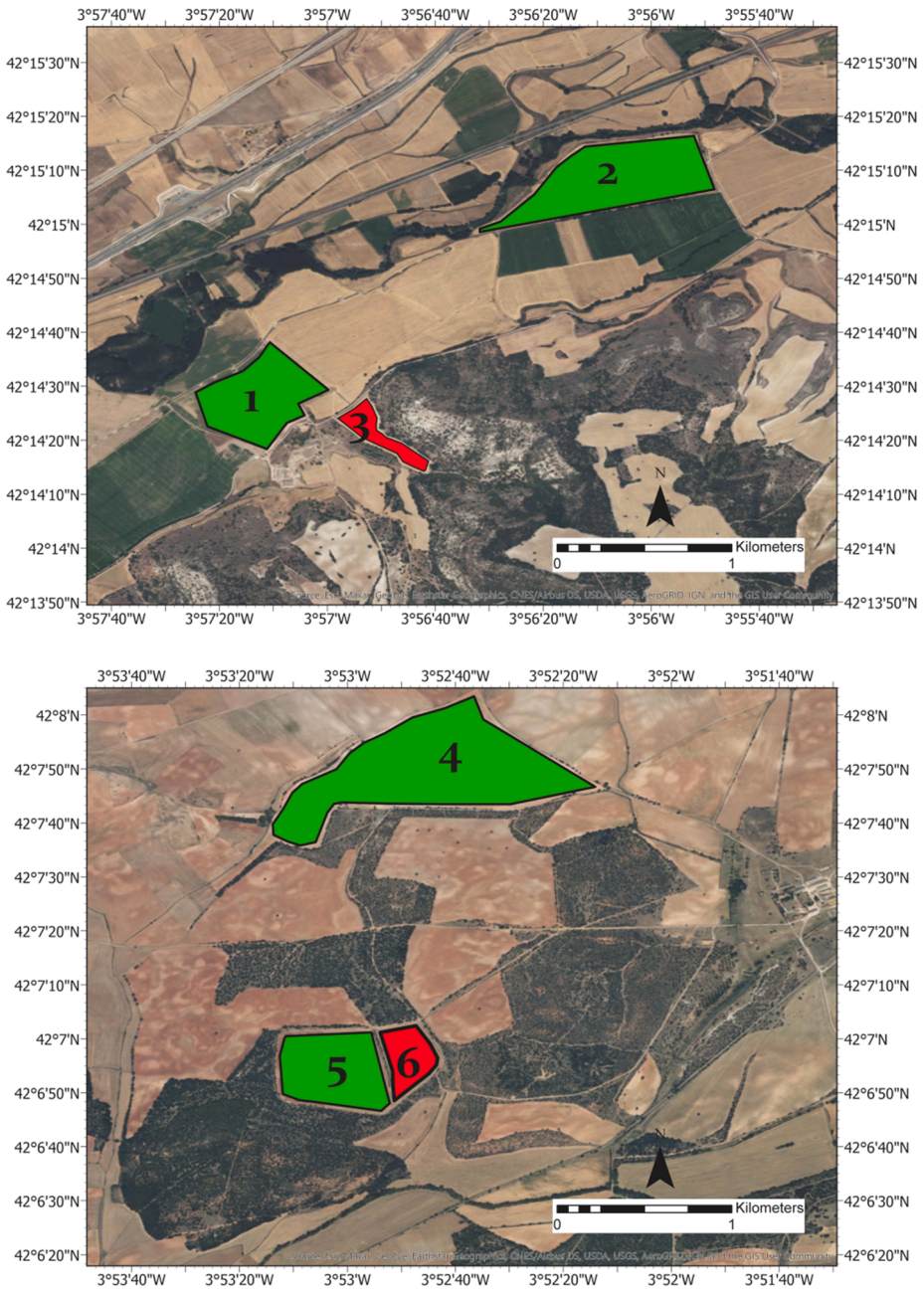

Fig. 2. Locations of the fields used in the study during season 2017–2019. Six fields are shown, two of them were used in alternate seasons, and the reference number for each field is indicated. Fields used independently for validation of the GY estimation model are highlighted in red, those used for training are in green. (For interpretation of the references to color in this figure legend, the reader is referred to the web version of this article.)

et al., 2016). The RF algorithm is a ML method developed by (Breinman, 2001), where the set of predictors is randomly distributed at each split, while the variables randomly selected at each split is a user-defined parameter as well as the number of trees. The optimal parameters regarding the number of trees and the number of variables randomly sampled as candidates at each split was optimized to 300 and 6 respectively. In this case the package "RandomForest" was used in R (R Core Team, 2021).

Support vector machine (SVM) used in regressions (Vapnik, 2013) is a ML approach that has also been used in agriculture for grain yield estimation (Oguntunde et al., 2018; Saruta et al., 2013). In R (R Core Team, 2021) the package "e1071" was used for the SVM in eps-regression, and the degree parameter needed for kernel was set at 3. Generalized boosted regression (BR) are combinations of two techniques: decision tree algorithms and boosting methods (Freund et al., 1999; Friedman, 2001). These approaches have been successfully used in grain yield estimation (Arumugam et al., 2021; Zhang et al., 2019). In R (R Core Team, 2021) package "gbm" was used, the number of trees was optimized at 5000 and the interaction depth at 5.

For all ML approaches, a 70% of the dataset (13,685 pixels) was used to train the models and a 30% of the dataset (6439 pixels) containing two fields not used in the training were used for validation. Fig. 6 shows the distribution of the data set, as density due to the different number of pixels in each set. We assume the distribution of data is equivalent in train and validation sets. Both training and validation datasets followed a similar distribution of data (Fig. 6). The accuracy assessment was carried out by calculating R^2, RMSE (eq. (1)) and actual GY MEAN (eq. (2)) to derive the % RMSE (eq. (3)) of the validation dataset.

Table 1
Sentinel-2 multispectral instrument information.

Band	Spatial Resolution (m)	Central Wavelength (nm)
B1: Coastal Aerosol	60	443
B2: Blue	10	490
B3: Green	10	560
B4: Red	10	665
B5: Red-Edge	20	705
B6: Red-Edge	20	740
B7: Red-Edge	20	783
B8: NIR	10	842
B8A: Vegetation RE	20	865
B9: Water Vapour	60	945
B10: SWIR Cirrus	60	1375
B11: SWIR	20	1610
B12: SWIR	20	2190

Table 2
The calculated vegetation indices and biophysical parameters.

Abbreviation	Parameter	Calculation	Reference
NDVI	Vegetation index	$\frac{B8-B4}{B8+B4}$	(Rouse Lr. et al., 1974)
GNDVI	Vegetation index	$\frac{B8-B3}{B8+B3}$	(Gitelson et al., 1996)
EVI	Vegetation index	$2.5\frac{B8-B4}{(B8-6\bullet B4-7.5\bullet B2)+1}$	(Haboudane et al., 2002)
RVI	Vegetation index	$\frac{B8}{B4}$	(Tucker, 1979)
TGI	Vegetation index	−0.5•(190•(B4-B3)-120•(B4-B2))	(Hunt et al., 2013)
NGRDI	Vegetation index	$\frac{(B3-B4)}{(B3+B4)}$	(Hunt et al., 2005)
CVI	Vegetation index	$\frac{B8\hat{A}\cdot B3}{B3\hat{A}\cdot B4}$	(Vincini et al., 2008)
LAI	Biophysical parameter	RTM on SNAP	(Weiss and Baret, 2016)

$$RMSE = \sqrt{\frac{\sum_{i=1}^{n}(predicted_i - actual_i)^2}{n}} \quad (1)$$

$$\text{MEAN} = \frac{\sum_{i=1}^{n} actual_i}{n} \quad (2)$$

$$\%RMSE = \frac{RMSE}{MEAN}\bullet 100 \quad (3)$$

3. Results

3.1. Machine learning approaches

The ML approach that produced higher R^2 and lower %RMSE is RF regression (Fig. 7), followed by BR and SVM. All machine learning approaches had better results in comparison with the baseline, multilinear regression (Table 3). For all phenological stages and indices, RF regression averaged between a highest $R^2 = 0.89$ and %RMSE = 15.4 and a lowest of $R^2 = 0.83$ and %RMSE = 19.1; meanwhile BR averaged between a highest $R^2 = 0.85$ and %RMSE = 18.3 and a lowest of $R^2 = 0.81$ and %RMSE = 20.7; SVM averaged between a highest $R^2 = 0.84$ and %RMSE = 19.1 and a lowest of $R^2 = 0.74$ and %RMSE = 23.7. The multilinear regression as baseline averaged between a highest $R^2 = 0.69$ and %RMSE = 26.8 and a lowest of $R^2 = 0.37$ and %RMSE = 35.7.

3.2. Phenology and date

Multidate Sentinel-2 imagery improved all data feeding instances here studied. There is a slightly improved result when using Sentinel-2 timeseries, rather than stem elongation and heading/anthesis phenological stages alone. In general terms, with single date images, heading/anthesis phenological stage performed slightly better in comparison with stem elongation (Table 3). In the case of RF regression, for instance, at stem elongation R^2 ranged between 0.83 and 0.84 and %RMSE

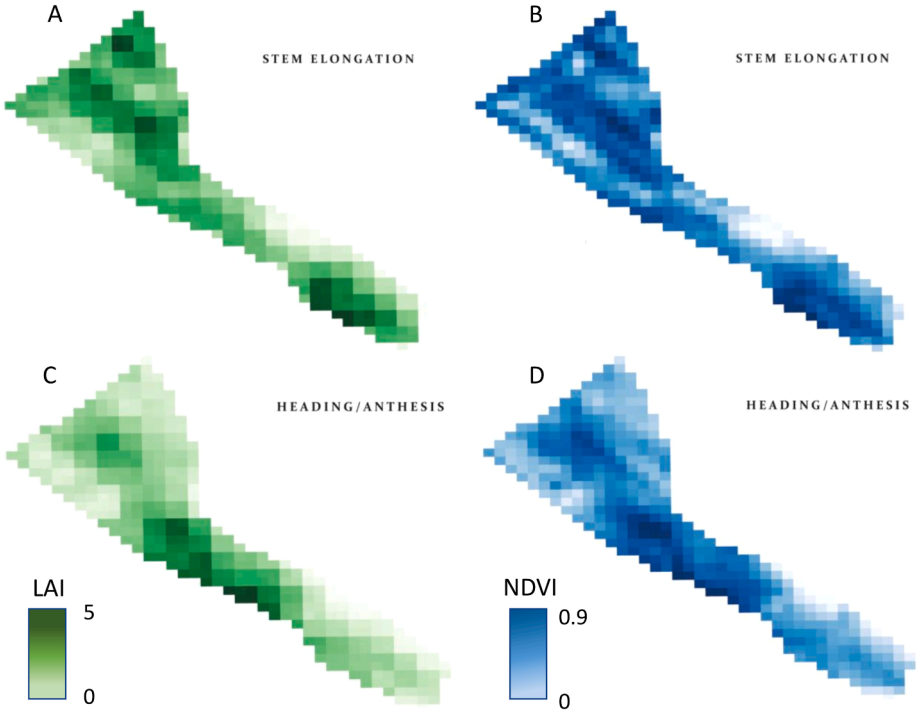

Fig. 3. Overview of LAI (in green A and C) and NDVI (in blue B and D) calculated from the Sentinel-2 images, with Field 3 as an example of the model validation with the two phenological stages studied, stem elongation at the top of the Figure (A and B) and heading/anthesis at the bottom (C and D). (For interpretation of the references to color in this figure legend, the reader is referred to the web version of this article.)

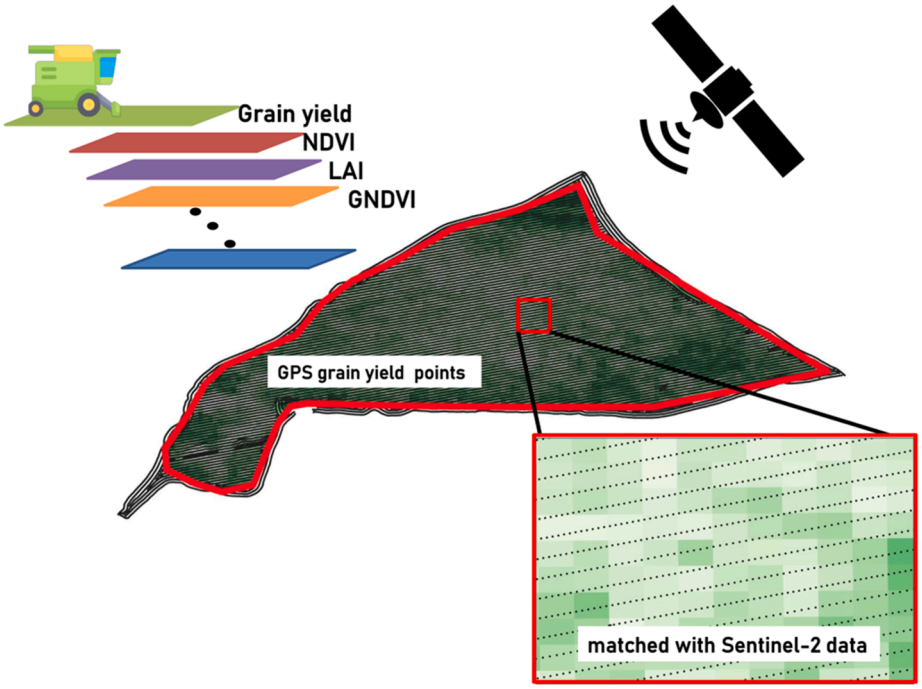

Fig. 4. Explanation of the distribution of yield points obtained with the combine harvester. Fields were manually buffered to avoid edge effects. The interpolation of GPS yield points to Sentinel-2 derived data is also shown.

18.3–19.1. Meanwhile at heading/anthesis, R^2 ranged between 0.86 and 0.88 and %RMSE 16.8–17.0. Finally, when using the whole timeseries, R^2 ranged between 0.87 and 0.89 and %RMSE 15.4–16.2. Hence, the estimation of within-field grain yield has a slightly improve when combining sensing dates.

3.3. Vegetation indices and biophysical parameters

In Fig. 7 a linear regression between the observed and estimated values at validation using multidate LAI data is shown. A higher density of points is observed around 3 to 6 t/ha as most sampled points were around these values. The linearity of the results is evident, yet the density of points is slightly uneven due to the nature of the data obtained in this area. The results suggest that with RF regression LAI using stem elongation and heading/anthesis dates together has the best performance ($R^2 = 0.89$ and %RMSE = 15.4). However, for the same specific situation VIs ($R^2 = 0.87$ and %RMSE = 16.2) and 10 m resolution Sentinel-2 bands ($R^2 = 0.88$ and %RMSE = 15.8) performed relatively well too. This trend was also observed for the rest of machine learning approaches here studied. Therefore, within-field wheat GY variability can be estimated relatively accurately with all the data feeding approaches here studied (vegetation indices, LAI and 10 m Sentinel-2 bands alone) being LAI the most accurate.

Regarding the vegetation indices alone (Table 4), we observed that RF regression yielded the best results. Support vector machine had more limited results and linear regression showed unacceptable %RMSE. With RF regression and multidate data, RVI, GNDVI and NDVI had the lowest %RMSE (16.2 in all the cases) as well as the highest R^2 (0.87 in all the cases). Greenness sensitive indices such as TGI or CVI had lower R^2 (0.85) and higher %RMSE (17.4) in contrast with the previous biomass sensitive indices.

RF regression is the most promising ML approach when using LAI derived from Sentinel-2 data processing. The use of all available dates also improved the results. Within-field relative accuracy can be observed in Fig. 8, where a comparison between observed and estimated wheat GY using LAI data is shown. The pixels shown in the two fields are validation pixels, two independent fields of the 30% not used for training the model; therefore, these present an independent visual validation of the accuracy of the developed model. Moreover, they reflect comparable general patterns of wheat GY within-field variability.

4. Discussion

This study is structured around three questions that cover three relevant factors for within-field GY variability mapping, with a central relevance in remote sensing for precision farming. First, we determined what Sentinel-2 derived data is more accurate to estimate within-field GY. Second, we analysed how relevant is the temporal variable of the information that is sensed, namely the potential of phenological stages assessment. And third, we inferred what modelling approach, weather simple linear regressions or more complex ML approaches, work best. Finally, we discuss the scope of the findings presented here in regard to precision farming.

4.1. Sentinel-2 data

Coming back to question one (What processing or combination of Sentinel-2 derived spectral information is more suitable to estimate within-field wheat GY?) we observed that the biophysical parameter LAI had a slightly improved performance in contrast with Sentinel-2 bands and VIs. The lower %RMSE (15.4) in the model derived from LAI in comparison with the one developed with VIs (16.2 %RMSE) is in line with other studies, which showed improved performance of LAI for estimating cereal (e.g. wheat) grain yield (Lambert et al., 2018; Zhou et al., 2020b). However, VIs constitute a simple approach to extract information from remotely sensed data and have been linked to crop yield features in the last years (Gracia-Romero et al., 2017; Liu et al., 2006; Segarra et al., 2020b). VIs are easy to use, yet the spectral information RTM can capture is more robust as it captures reflectance changes in crop stages and changing architectures (Viña et al., 2011), in this sense, LAI was calculated using RTM, which are able to capture improved information of crop canopies (Wolanin et al., 2019). Moreover, most indices experience saturation at certain crop stages (Bannari et al., 1995), although a combination of trait specific indices might

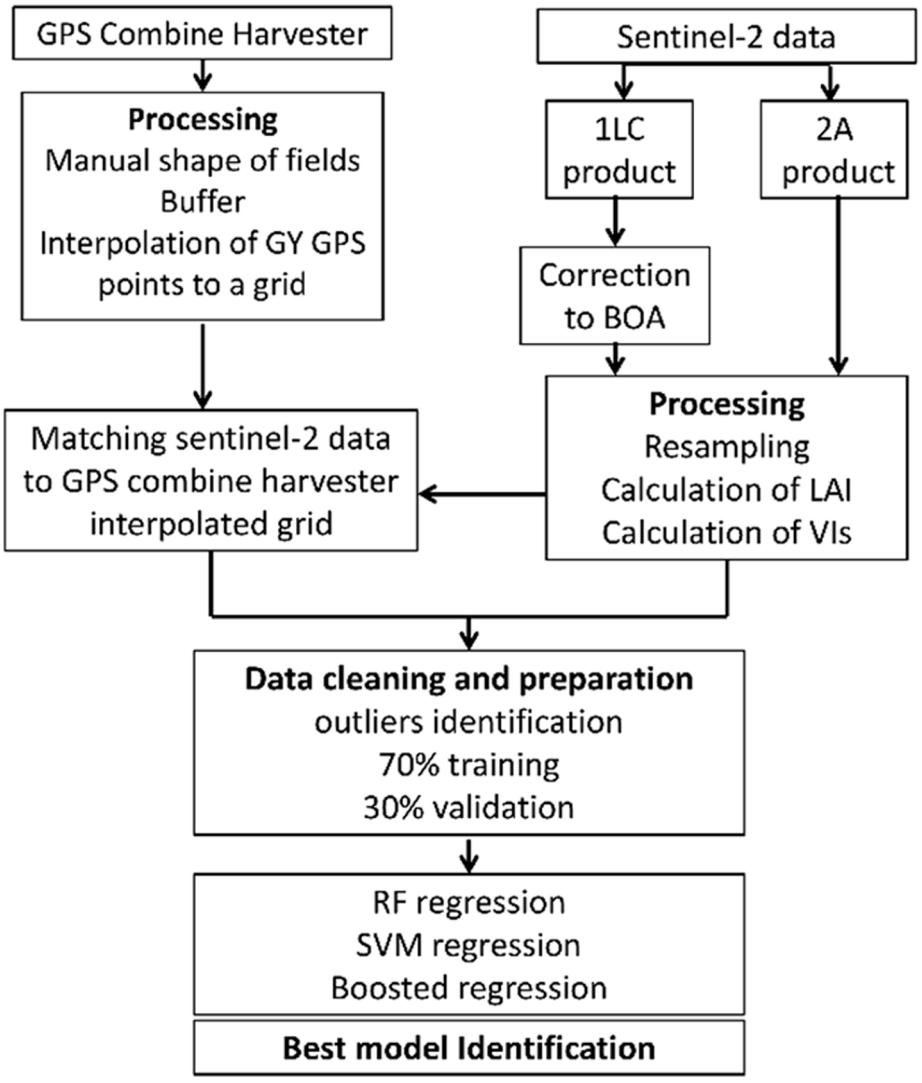

Fig. 5. Method overview of the process to estimate wheat GY using several data and ML approaches.

overcome this issue. Regarding Sentinel-2 bands alone, there is still a slightly improvement of GY models when using LAI (%RMSE 15.4) than bands alone (%RMSE 15.8). Other authors (Hunt et al., 2019a) argued that ML algorithms extract the most from the spectral information due to their capacity to capture complex interactions among variables, and therefore are successfully linked with within-field GY. Nonetheless, on top of this, we can argue that hybrid models that use advanced RTMs to describe biophysical parameters such as LAI and subsequently are matched to GY to feed ML models can even improve and add robustness to the models. These approaches have mainly been used in phenotyping (Jin et al., 2021), but as observed here can be almost operational for use in within-field wheat GY estimation.

4.2. Time series and phenology

Regarding question two (Can wheat GY models matching phenological stages be accurate and have potential to be applied in precision agriculture?) we observed that multi-date data improves the capacity to estimate within-field grain yield variability. In all three data feeding instances (Sentinel-2 bands, LAI and VIs), R^2 was higher and RMSE lower when using multi-date Sentinel-2 data (Table 3). Yet, the full temporal resolution of Sentinel-2 images could not be exploited as the availability of images for the regions studied was limited throughout the three seasons due to cloud cover. Despite of the limitations, several images throughout the season could be analysed following the phenological stages stem elongation and heading/anthesis. Interestingly, LAI assessed at stem elongation and heading/anthesis predicted better GY (lower %RMSE) than VIs and Sentinel-2 bands. This is coherent with the fact that LAI is a good indicator of potential canopy photosynthesis, with these reproductive stages being crucial in defining yield (Miralles et al., 2000; Villegas, 2001). In the case of the VIs and eventually of the single bands they may reflect later (during the crop cycle); particularly in terms of stay green and the onset of crop senescence during grain filling (Aparicio et al., 2000). Decrease in Stay Green, as response for example of water stress or lack of mineral nutrients effects may affect GY through an accelerated reduction of photosynthetic assimilates during the grain filling (Christopher et al., 2016), which might be too late for a reasoned management (e.g. additional irrigation or top-dressing fertilization). Moreover, LAI and VIs in wheat are frequently weakly correlated, which means their performance predicting yield are not necessarily comparable (Serrano et al., 2000). In this sense, for single phenological stages, the efficiency of the models was relatively high. Hence the estimation of GY before the whole season is completed, around March to May can help farmers to guide management decisions and ensure a better harvest. Several authors have matched Sentinel-2 images with phenology to estimate wheat GY at various resolutions (Fieuzal et al., 2020; Segarra et al., 2020b; Toscano et al., 2019) that allows an improved opportunity for precision farming management. The technical progress of Sentinel-2

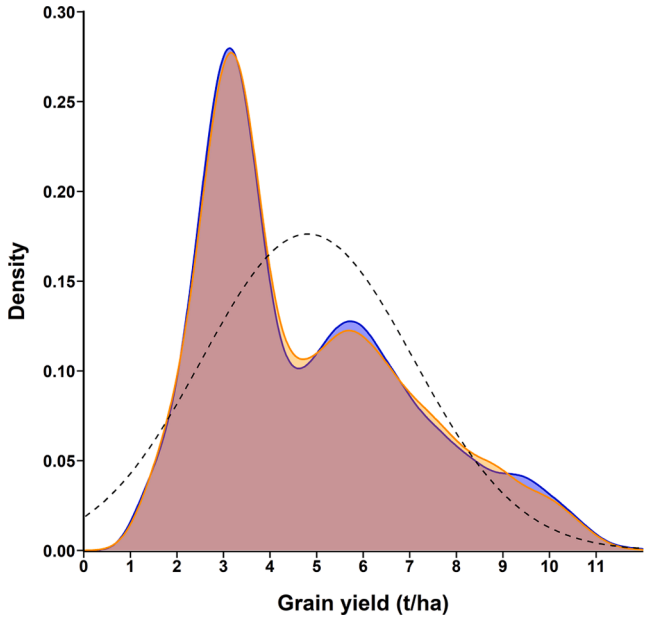

Fig. 6. Datasets distribution, orange shading indicates data forming the test set, blue shading the data forming the training set. The dotted line indicates a theoretical perfect normal distribution. (For interpretation of the references to color in this figure legend, the reader is referred to the web version of this article.)

and the increasing development of modelling approached for GY estimation now makes precision farming affordable and cost-effective and thus, almost operational (Weiss et al., 2020).

4.3. Modelling approaches

Regarding the third question (Which ML approach is more suitable for high resolution crop-specific wheat GY modelling?) we observed that RF clearly outperformed BR, SVM and multilinear regression (Table 4). In contrast with this, other authors (Heremans et al., 2015) observed an improved performance of BR in comparison with RF regression, when using VIs. Nonetheless, we can argue that the findings of this article show RF as an improved modelling approach when using LAI to estimate within field grain yield, as discussed previously. In contrast with other authors who did not find improvements between simple linear regressions and ML (Uno et al., 2005; Zhou et al., 2020a), we found that the relationship between crop yield and reflectance is complex enough for ML approaches and results in improvements in within-field yield predictions. RF is less prone to outliers, and hence one would expect yield estimation performance to increase, as we have corroborated here. Besides, RF algorithm is powerful in handling both linear and non-linear relationship as wheat yield and spectral information might have some non-linearity (Kumhálová and Matějková, 2017; Tesfaye et al., 2021). In general, we observed that the modelling approach is central for an effective GY estimation. We can argue that the modelling is the most important factor, followed by the sensing date (timeseries availability importantly linked to phenology) and the processing of the spectral data (LAI, for instance). In an equivalent study developed in the UK, RF was also used and compared to simple regression but no other machine learning approaches were presented (Hunt et al., 2019a). The results here obtained confirm the effectiveness of RF regression to estimate within-field GY variability using Sentinel-2 imagery for the case of Spain. Nonetheless, a further research and comparison of ML approaches could be developed aiming to standardize methodologies for specific regions and crop-specific cases for this almost operational precision agriculture technology. The ability of RF to cope with multivariate relationships between data of different types and resolutions is a key advantage over methods such as linear regression, which can only address univariate relationships.

4.4. Precision farming

To our knowledge, hitherto advanced models using ML approaches to estimate within-field GY in cereals have focused on demonstrations (Hunt et al., 2019a; Kayad et al., 2019) of single machine learning models and VIs or simple regressions (Cavalaris et al., 2021). Overall, there are a handful of articles (only two focused on bread wheat and none on durum wheat) dealing with GPS combine harvester and Sentinel-2 images and none have assessed several ML approaches, spectral indices and biophysical parameters retrieved from RTM. Hence, the results here presented assessing several ML approaches and Sentinel-2 data processing approaches are a novelty for this growing research

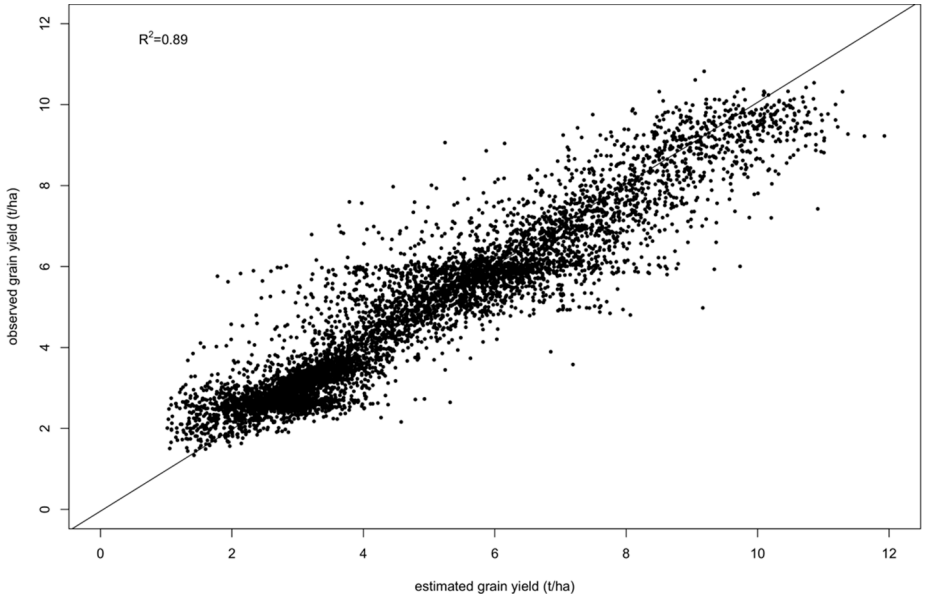

Fig. 7. Regression between observed and estimated-GY relative values at validation using RF regression, LAI data) and the whole timeseries combined. The black line indicates perfect correlation.

Table 3
At validation, model accuracies achieved for the various sensing periods and indices with random forest regression, support vector machine, boosted regression and baseline multilinear regression. S2 refers to Sentinel-2, while RMSE stands for root mean square error.

			Random Forest			Support Vector Machine			Boosted Regression			Multilinear regression		
S2 date	**Phenological stages**	**data**	**R^2**	**RMSE (t/ha)**	**% RMSE**	**R^2**	**RMSE (t/ha)**	**% RMSE**	**R^2**	**RMSE (t/ha)**	**% RMSE**	**R^2**	**RMSE (t/ha)**	**% RMSE**
March/April	Stem elongation	VIs	0.83	0.92	19.1	0.74	1.11	23.0	0.82	0.96	19.9	0.61	1.33	27.6
		LAI	0.84	0.84	17.4	0.72	1.09	22.6	0.84	0.82	17.1	0.47	1.73	35.9
		10 m S2	0.84	0.88	18.3	0.76	1.14	23.7	0.81	1.00	20.7	0.53	1.57	32.6
May		VIs	0.86	0.82	17.0	0.80	0.99	20.5	0.84	0.92	19.1	0.54	1.41	29.3
	Heading/Anthesis	LAI	0.88	0.76	15.8	0.81	1.01	20.9	0.82	1.01	21.0	0.38	1.86	38.6
		10 m S2	0.86	0.81	16.8	0.81	1.09	22.6	0.82	0.97	20.1	0.37	1.72	35.7
March/April + May/ June	Stem elongation + Heading/Anthesis	VIs	0.87	0.78	16.2	0.82	0.89	18.5	0.84	0.91	18.9	0.69	1.29	26.8
		LAI	0.89	0.74	15.4	0.84	0.92	19.1	0.85	0.88	18.3	0.48	1.74	36.1
		10 m S2	0.88	0.76	15.8	0.83	0.91	18.9	0.83	0.94	19.5	0.58	1.49	30.9

Table 4
Testing of single vegetation indices for all the analysed dates together.

		Random Forest		Support Vector Machine			Boosted Regression			Linear regression		
Vegetation index	**R^2**	**RMSE (t/ha)**	**%RMSE**	**R^2**	**RMSE (t/ha)**	**%RMSE**	**R^2**	**RMSE (t/ha)**	**%RMSE**	**R^2**	**RMSE (t/ha)**	**%RMSE**
GNDVI	0.87	0.78	16.2	0.78	1.00	20.7	0.83	0.79	16.4	0.47	1.60	33.2
NDVI	0.87	0.78	16.2	0.79	0.98	20.3	0.83	0.79	16.4	0.53	1.56	32.4
EVI	0.84	0.81	16.8	0.77	1.02	21.2	0.81	0.81	16.8	0.56	1.44	29.9
RVI	0.87	0.78	16.2	0.78	1.03	21.4	0.83	0.79	16.4	0.51	1.56	32.4
TGI	0.85	0.84	17.4	0.74	1.20	24.9	0.83	0.82	17.0	0.37	1.75	36.3
NGRDI	0.85	0.79	16.4	0.75	1.05	21.8	0.84	0.79	16.4	0.55	1.55	32.2
CVI	0.85	0.84	17.4	0.74	1.24	25.7	0.83	0.81	16.8	0.37	1.77	36.7

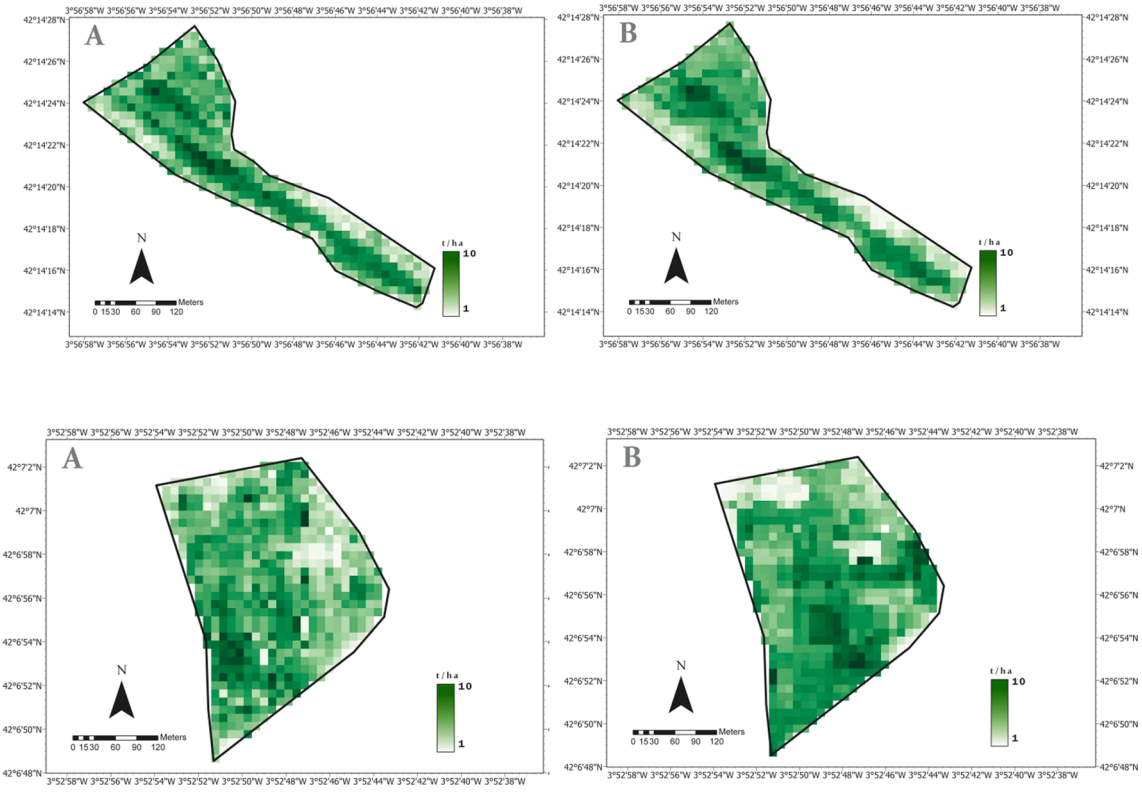

Fig. 8. Comparison between actual GY pixels (A) and estimated GY with the independent validation dataset (B) in the field 3 (top) and 6 (bottom) using random forest regression and LAI data derived from RTM and Sentinel-2 data.

field. In this sense, we believe that the methodology here developed, and the results obtained can contribute to precision farming. First, the ML approaches analysed present RF as an efficient model to monitor within-field wheat GY. The use of ML to retrieve GY has been considered one of the most important areas develop associated with remote sensing and agriculture (Weiss et al., 2020). On top of that, based on the results, we can argue that retrieving biophysical parameters with RTM that can be linked to crop traits and subsequently used for ML models is a step forward in precision agriculture. The usage of RTMs with ML regression algorithms is opening up a powerful and promising field of vegetation properties retrieval from EOS data (Berger et al., 2020; Estévez et al., 2020), but has yet to be fully explored in precision agriculture. LAI, leaf structure parameters, leaf chlorophyll content, leaf carotenoid content, leaf anthocyanin content or leaf equivalent water thickness are, among others, traits of agricultural crops that can be retrieved from RTM (Danner et al., 2021). The availability of biophysical processors in software such as SNAP of the European Space Agency used here opens a door to the applicability of these parameters. In this sense, with increased computing power available in the next years, RTM inversion can provide an elegant alternative to estimate fertilizer requirements in precision agriculture (Maes and Steppe, 2019). Furthermore, RTM have shown the potential of Sentinel-2 data to map disease-incidence dynamics in agriculture plots (Hornero et al., 2020). Regarding irrigation, cropland canopy water content thematic layers have been developed with RTM and Sentinel-2 imagery (Boren and Boschetti, 2020) using several parameters such as water thickness or dry matter content, among others.

In addition to this, the results obtained in this study with single image acquisition and its matching with phenological stage can help to locate low-yielding spots in croplands and subsequently apply precise farming decisions. In this sense, the performance of LAI and other biophysical parameters of interest for precision agriculture retrieved from RTM could contribute to find physiological or agronomic explanations and apply reasoned managements. Our study also has some limitations to overcome such as its applicability in other crops and in different agroclimates.

We believe that a way to implement the adoption of precision farming for wheat in the inner Mediterranean/continental regions of Spain following these findings would be:

1) Further expanding this study by increasing the geolocated dataset of GPS combine harvesters across different environmental and crop type conditions in Spain. This machinery is more accessible nowadays and is being applied more frequently now. Moreover, Spain, where this study takes places, meets a wide range of climatic conditions and crop types with relevance to European agricultural systems.
2) Based on our results, RF regression is the most suitable modelling approach to estimate within-field GY at different growing stage and can serve as a starting point to further develop streamlined and standardized models
3) Biophysical parameters retrievable with RTM such as LAI, leaf structure parameters, leaf chlorophyll content, leaf carotenoid content, leaf anthocyanin content or leaf equivalent water thickness, among others, could be used as explanatory variables to understand limitations in specific field spots and guide the application of adequate management strategies (smart fertilization, regeneration of degraded soils, etc.). These parameters can be relevant to physiologically and agronomic-related crop performances at each phenological stages.
4) The public agricultural institutions of the country together with farmers could lead the creation of an openly accessible platform to estimate within field wheat GY and guide specific management decision for farmers with this information. Following the example of Belgium and the platform WatchItGrow (Curnel, 2017) to monitor potato yield with Sentinel-2 data.

5. Conclusions

This article studied the performance of Sentinel-2 derived spectral information, EOS Sentinel-2 multi-date images, and machine learning approaches to define the most effective parameters for within-field GY variability mapping. To our knowledge, no study has focused on the use of biophysical parameters (LAI) retrieved from RTM and a complete set of VIs as training data for high resolution wheat GY estimation as they have in general terms focused on few VIs or spectral bands alone. As most studies focus on field to regional scale GY estimation, only a scarce number of studies have focused on within-field wheat GY. Hence, this study contributes with novel methodological advancements in within-field wheat GY estimation (and to the best of our knowledge none in durum wheat) with implications in precision farming. When comparing the individual performances of different categories of parameters (LAI versus VIs / single bands) assessed at a given phenological stage we found that each category of traits best predicted GY at a different phenological stage, which may have also practical applications for precision agriculture. We found that the modelling approach (specifically RF in our study) is the most relevant factor for GY estimation, followed by the sensing date (single date or multi-date time series) and finally the Sentinel-2 derived information (biophysical parameters, vegetation indices or band alone). At the best performing scenario RF regression with the whole phenological images available the model reached and R^2 of 0.89 and a % RMSE of 15.4, which we can consider a relatively high performing model. Understanding wheat GY variability within a field and applying precision farming management practices is central for environmental, agricultural, and socioeconomic sustainability.

CRediT authorship contribution statement

Joel Segarra: Conceptualization, Data curation, Formal analysis, Investigation, Methodology, Project administration, Validation, Visualization. **Jose Luis Araus:** Funding acquisition, Resources, Supervision, Writing – original draft, Writing – review & editing. **Shawn C. Kefauver:** Conceptualization, Project administration, Resources, Supervision.

Declaration of Competing Interest

The authors declare that they have no known competing financial interests or personal relationships that could have appeared to influence the work reported in this paper.

Acknowledgements

We acknowledge the support of the project PID2019-106650RB-C21 from the Ministerio de Ciencia e Innovación, Spain. J.S. is a recipient of a FPI doctoral fellowship from the same institution (grant: PRE2020-091907). J.L.A. acknowledges support from the Institució Catalana de Recerca i Estudis Avançats (ICREA), Generalitat de Catalunya, Spain). S. C.K. is supported by the Ramon y Cajal RYC-2019-027818-I research fellowship from the Ministerio de Ciencia e Innovación, Spain. We acknowledge the support of Cerealto Siro Group, together with Cristina de Diego and Javier Velasco, technical staff from the company, by providing the wheat yield data. This research was also supported by the COST Action CA17134 SENSECO (Optical synergies for spatiotemporal sensing of scalable ecophysiological traits) funded by COST (European Cooperation in Science and Technology, www.cost.eu).

References

Aparicio, N., Villegas, D., Casadesus, J., Araus, J.L., Royo, C., 2000. Spectral vegetation indices as nondestructive tools for determining durum wheat yield. Agron. J. 92 (1), 83–91. https://doi.org/10.2134/agronj2000.92183x.

Arumugam, P., Chemura, A., Schauberger, B., Gornott, C., 2021. Remote sensing based yield estimation of rice (Oryza sativa l.) using gradient boosted regression in India. Remote Sens. 13, 1–18. https://doi.org/10.3390/rs13122379.
Bach, H., Mauser, W., 2018. Sustainable agriculture and smart farming. In: Earth Observation Open Science and Innovation. Springer, Cham, pp. 261–269. https://doi.org/10.1007/978-3-319-65633-5_12.
Bannari, A., Morin, D., Bonn, F., Huete, A.R., 1995. A review of vegetation indices. Remote Sens. Rev. 13 (1-2), 95–120. https://doi.org/10.1080/02757259509532298.
Berger, K., Verrelst, J., Féret, J.-B., Hank, T., Wocher, M., Mauser, W., Camps-Valls, G., 2020. Retrieval of aboveground crop nitrogen content with a hybrid machine learning method. Int. J. Appl. Earth Obs. Geoinf. 92, 102174. https://doi.org/10.1016/j.jag.2020.102174.
Boren, E.J., Boschetti, L., 2020. Landsat-8 and sentinel-2 canopy water content estimation in croplands through radiative transfer model inversion. Remote Sens. 12, 2803. https://doi.org/10.3390/rs12172803.
Breinman, L., 2001. Random forest. Mach. Learn. https://doi.org/10.1023/A:1010933404324.
Bzdok, D., Altman, N., Krzywinski, M., 2018. Points of significance: statistics versus machine learning. Nat. Methods 15 (4), 233–234. https://doi.org/10.1038/nmeth.4642.
Cavalaris, C., Megoudi, S., Maxouri, M., Anatolitis, K., Sifakis, M., Levizou, E., Kyparissis, A., 2021. Modeling of durum wheat yield based on sentinel-2 imagery. Agronomy 11 (8), 1486. https://doi.org/10.3390/agronomy11081486.
Chlingaryan, A., Sukkarieh, S., Whelan, B., 2018. Machine learning approaches for crop yield prediction and nitrogen status estimation in precision agriculture: A review. Computers and electronics in agriculture 151, 61–69. https://doi.org/10.1016/j.compag.2018.05.012.
Christopher, J.T., Christopher, M.J., Borrell, A.K., Fletcher, S., Chenu, K., 2016. Stay-green traits to improve wheat adaptation in well-watered and water-limited environments. J. Exp. Bot. 67 (17), 5159–5172. https://doi.org/10.1093/jxb/erw276.
Curnel, Y., 2017. Watch It Grow, an innovative platform for a sustainable growth of the Belgian potato production, FACCE MACSUR Reports.
Danner, M., Berger, K., Wocher, M., Mauser, W., Hank, T., 2021. Efficient RTM-based training of machine learning regression algorithms to quantify biophysical & biochemical traits of agricultural crops. ISPRS J. Photogramm. Remote Sens. 173, 278–296. https://doi.org/10.1016/j.isprsjprs.2021.01.017.
Duan, B.o., Fang, S., Gong, Y., Peng, Y.i., Wu, X., Zhu, R., 2021. Remote estimation of grain yield based on UAV data in different rice cultivars under contrasting climatic zone. F. Crop. Res. 267, 108148. https://doi.org/10.1016/j.fcr.2021.108148.
Estévez, J., Vicent, J., Rivera-Caicedo, J.P., Morcillo-Pallarés, P., Vuolo, F., Sabater, N., Camps-Valls, G., Moreno, J., Verrelst, J., 2020. Gaussian processes retrieval of LAI from Sentinel-2 top-of-atmosphere radiance data. ISPRS J. Photogramm. Remote Sens. 167, 289–304. https://doi.org/10.1016/j.isprsjprs.2020.07.004.
Fieuzal, R., Bustillo, V., Collado, D., Dedieu, G., 2020. Combined use of multi-temporal Landsat-8 and sentinel-2 images for wheat yield estimates at the intra-plot spatial scale. Agronomy 10 (3), 327. https://doi.org/10.3390/agronomy10030327.
Foley, J.A., Ramankutty, N., Brauman, K.A., Cassidy, E.S., Gerber, J.S., Johnston, M., Mueller, N.D., O'Connell, C., Ray, D.K., West, P.C., Balzer, C., Bennett, E.M., Carpenter, S.R., Hill, J., Monfreda, C., Polasky, S., Rockström, J., Sheehan, J., Siebert, S., Tilman, D., Zaks, D.P.M., 2011. Solutions for a cultivated planet. Nature 478 (7369), 337–342. https://doi.org/10.1038/nature10452.
Font Tullot, I., 2000. Climatología de España y Portugal. Universidad de Salamanca, Salamanca.
Freund, Y., Schapire, R., Abe, N., 1999. A short introduction to boosting. J.-Japanese Soc. Artif. Intell. 1612, 771–780.
Friedman, J.H., 2001. Greedy function approximation: a gradient boosting machine. Ann. Stat. 1189–1232. https://doi.org/10.1214/aos/1013203451.
García-Escudero, L.A., Gordaliza, A., Matrán, C., Mayo-Iscar, A., 2008. A general trimming approach to robust cluster analysis. Ann. Stat. 36, 1324–1345. https://doi.org/10.1214/07-AOS515.
Gilardelli, C., Stella, T., Confalonieri, R., Ranghetti, L., Campos-Taberner, M., García-Haro, F.J., Boschetti, M., 2019. Downscaling rice yield simulation at sub-field scale using remotely sensed LAI data. Eur. J. Agron. 103, 108–116. https://doi.org/10.1016/j.eja.2018.12.003.
Gitelson, A.A., Kaufman, Y.J., Merzlyak, M.N., 1996. Use of a green channel in remote sensing of global vegetation from EOS- MODIS. Remote Sens. Environ. 58 (3), 289–298. https://doi.org/10.1016/S0034-4257(96)00072-7.
Gracia-Romero, A., Kefauver, S.C., Vergara-Díaz, O., Zaman-Allah, M.A., Prasanna, B.M., Cairns, J.E., Araus, J.L., 2017. Comparative performance of ground vs. Aerially assessed rgb and multispectral indices for early-growth evaluation of maize performance under phosphorus fertilization. Front. Plant Sci. 8, 1–13. https://doi.org/10.3389/fpls.2017.02004.
Haboudane, D., Miller, J.R., Tremblay, N., Zarco-Tejada, P.J., Dextraze, L., 2002. Integrated narrow-band vegetation indices for prediction of crop chlorophyll content for application to precision agriculture. Remote Sens. Environ. 81 (2-3), 416–426. https://doi.org/10.1016/S0034-4257(02)00018-4.
Heremans, S., Dong, Q., Zhang, B., Bydekerke, L., Van Orshoven, J., 2015. Potential of ensemble tree methods for early-season prediction of winter wheat yield from short time series of remotely sensed normalized difference vegetation index and in situ meteorological data. J. Appl. Remote Sens. 9 (1), 097095. https://doi.org/10.1117/1.JRS.9.097095.
Hornero, A., Hernández-Clemente, R., North, P.R.J., Beck, P.S.A., Boscia, D., Navas-Cortes, J.A., Zarco-Tejada, P.J., 2020. Monitoring the incidence of Xylella fastidiosa infection in olive orchards using ground-based evaluations, airborne imaging spectroscopy and Sentinel-2 time series through 3-D radiative transfer modelling. Remote Sens. Environ. 236, 111480. https://doi.org/10.1016/j.rse.2019.111480.
Hunt, E.R., Cavigelli, M., Daughtry, C.S.T., Mcmurtrey, J.E., Walthall, C.L., 2005. Evaluation of digital photography from model aircraft for remote sensing of crop biomass and nitrogen status. Precis. Agric. 6 (4), 359–378. https://doi.org/10.1007/s11119-005-2324-5.
Hunt, E.R., Doraiswamy, P.C., McMurtrey, J.E., Daughtry, C.S.T., Perry, E.M., Akhmedov, B., 2013. A visible band index for remote sensing leaf chlorophyll content at the Canopy scale. Int. J. Appl. Earth Obs. Geoinf. 21, 103–112. https://doi.org/10.1016/j.jag.2012.07.020.
Hunt, M.L., Blackburn, G.A., Carrasco, L., Redhead, J.W., Rowland, C.S., 2019. High resolution wheat yield mapping using Sentinel-2. Remote Sens. Environ. 233, 111410. https://doi.org/10.1016/j.rse.2019.111410.
Hunt, M.L., Blackburn, G.A., Rowland, C.S., 2019b. Monitoring the sustainable intensification of arable agriculture: the potential role of earth observation. Int. J. Appl. Earth Obs. Geoinf. 81, 125–136. https://doi.org/10.1016/j.jag.2019.05.013.
Jeong, J.H., Resop, J.P., Mueller, N.D., Fleisher, D.H., Yun, K., Butler, E.E., Timlin, D.J., Shim, K.M., Gerber, J.S., Reddy, V.R., Kim, S.H., 2016. Random forests for global and regional crop yield predictions. PLoS One 11, 1–15. https://doi.org/10.1371/journal.pone.0156571.
Jin, X., Zarco-Tejada, P.J., Schmidhalter, U., Reynolds, M.P., Hawkesford, M.J., Varshney, R.K., Yang, T., Nie, C., Li, Z., Ming, B., Xiao, Y., Xie, Y., Li, S., 2021. High-throughput estimation of crop traits: a review of ground and aerial phenotyping platforms. IEEE Geosci. Remote Sens. Mag. 9, 200–231. https://doi.org/10.1109/MGRS.2020.2998816.
Kayad, A., Sozzi, M., Gatto, S., Marinello, F., Pirotti, F., 2019. Monitoring within-field variability of corn yield using sentinel-2 and machine learning techniques. Remote Sens. 11 https://doi.org/10.3390/rs11232873.
Kumhálová, J., Matějková, Š., 2017. Yield variability prediction by remote sensing sensors with different spatial resolution. Int. Agrophys. 31, 195–202. https://doi.org/10.1515/intag-2016-0046.
Lambert, M.J., Traoré, P.C.S., Blaes, X., Baret, P., Defourny, P., 2018. Estimating smallholder crops production at village level from Sentinel-2 time series in Mali's cotton belt. Remote Sens. Environ. 216, 647–657. https://doi.org/10.1016/j.rse.2018.06.036.
Liu, L., Wang, J., Bao, Y., Huang, W., Ma, Z., Zhao, C., 2006. Predicting winter wheat condition, grain yield and protein content using multi-temporal EnviSat-ASAR and Landsat TM satellite images. Int. J. Remote Sens. 27, 737–753. https://doi.org/10.1080/01431160500296867.
Lyle, G., Bryan, B.A., Ostendorf, B., 2014. Post-processing methods to eliminate erroneous grain yield measurements: review and directions for future development. Precis. Agric. 15, 377–402. https://doi.org/10.1007/s11119-013-9336-3.
Maes, W.H., Steppe, K., 2019. Perspectives for remote sensing with unmanned aerial vehicles in precision agriculture. Trends Plant Sci. 24, 152–164. https://doi.org/10.1016/j.tplants.2018.11.007.
Migdall, S., Brüggemann, L., Bach, H., 2018. Earth observation in agriculture. In: Satellite-Based Earth Observation. Springer International Publishing, Cham, pp. 85–93. https://doi.org/10.1007/978-3-319-74805-4_9.
Miralles, D.J., Richards, R.A., Slafer, G.A., 2000. Duration of the stem elongation period influences the number of fertile florets in wheat and barley. Funct. Plant Biol. 27, 931. https://doi.org/10.1071/PP00021.
Mokhtari, A., Noory, H., Vazifedoust, M., 2018. Improving crop yield estimation by assimilating LAI and inputting satellite-based surface incoming solar radiation into SWAP model. Agric. For. Meteorol. 250–251, 159–170. https://doi.org/10.1016/j.agrformet.2017.12.250.
Oguntunde, P.G., Lischeid, G., Dietrich, O., 2018. Relationship between rice yield and climate variables in southwest Nigeria using multiple linear regression and support vector machine analysis. Int. J. Biometeorol. 62, 459–469. https://doi.org/10.1007/s00484-017-1454-6.
R Core Team, 2021. A language and environment for statistical computing.
Ranieri, R., 2015. Geography of the durum wheat crop. Pastaria Int (6), 24–36.
Rosegrant, M.W., Cline, S.A., 2003. Global food security: challenges and policies. Science (80-.) 302, 1917–1919. https://doi.org/10.1126/science.1092958.
Rouse Lr., J.W., Haas, R., Schell, J., Deering, D., 1974. Monitoring vegetation systems in the great plains with erts. NASA Spec. Publ. 351.
Saruta, K., Hirai, Y., Tanaka, K., Inoue, E., Okayasu, T., Mitsuoka, M., 2013. Predictive models for yield and protein content of brown rice using support vector machine. Comput. Electron. Agric. 99, 93–100. https://doi.org/10.1016/j.compag.2013.09.003.
Savary, S., Willocquet, L., Pethybridge, S.J., Esker, P., McRoberts, N., Nelson, A., 2019. The global burden of pathogens and pests on major food crops. Nat. Ecol. Evol. 3, 430–439. https://doi.org/10.1038/s41559-018-0793-y.
Segarra, J., Buchaillot, M.L., Araus, J.L., Kefauver, S.C., 2020a. Remote sensing for precision agriculture: sentinel-2 improved features and applications. Agronomy 1–18. https://doi.org/10.3390/agronomy10050641.
Segarra, J., González-Torralba, J., Aranjuelo, Í., Araus, J.L., Kefauver, S.C., 2020b. Estimating wheat grain yield using Sentinel-2 imagery and exploring topographic features and rainfall effects on wheat performance in Navarre. Spain. Remote Sens. 12, 1–24. https://doi.org/10.3390/rs12142278.
Serrano, L., Filella, I., Peñuelas, J., 2000. Remote sensing of biomass and yield of winter wheat under different nitrogen supplies. Crop Sci. 40, 723–731. https://doi.org/10.2135/cropsci2000.403723x.
Stas, M., Van Orshoven, J., Dong, Q., Heremans, S., Zhang, B., 2016. A comparison of machine learning algorithms for regional wheat yield prediction using NDVI time series of SPOT-VGT. In: 2016 5th Int. Conf. Agro-Geoinformatics, Agro-Geoinformatics, pp. 16–20. doi: 10.1109/Agro-Geoinformatics.2016.7577625.

Sutton, M.A., Howard, C.M., Erisman, J.W., Billen, G., Bleeker, A., Grennfelt, P., Van Grinsven, H., Grizzetti, B., 2011. The European nitrogen assessment: sources, effects and policy perspectives. Cambridge University Press. https://doi.org/10.1002/met.1290.

Tesfaye, A.A., Osgood, D., Aweke, B.G., 2021. Combining machine learning, space-time cloud restoration and phenology for farm-level wheat yield prediction. Artif. Intell. Agric. 5, 208–222. https://doi.org/10.1016/j.aiia.2021.10.002.

Toscano, P., Castrignanò, A., Di Gennaro, S.F., Vonella, A.V., Ventrella, D., Matese, A., 2019. A precision agriculture approach for durum wheat yield assessment using remote sensing data and yield mapping. Agronomy 9. https://doi.org/10.3390/agronomy9080437.

Tucker, C.J., 1979. Red and photographic infrared linear combinations for monitoring vegetation. Remote Sens. Environ. 8, 127–150. https://doi.org/10.1016/0034-4257(79)90013-0.

Uno, Y., Prasher, S.O., Lacroix, R., Goel, P.K., Karimi, Y., Viau, A., Patel, R.M., 2005. Artificial neural networks to predict corn yield from Compact Airborne Spectrographic Imager data. Comput. Electron. Agric. 47, 149–161. https://doi.org/10.1016/j.compag.2004.11.014.

van Ittersum, M.K., 2016. Crop yields and global food security. Will yield increase continue to feed the world? Eur. Rev. Agric. Econ. 43, 191–192. https://doi.org/10.1093/erae/jbv034.

Vapnik, V., 2013. The Nature of Statistical Learning Theory. Springer Science & Business Media. https://doi.org/10.1007/978-1-4757-3264-1_1.

Villegas, D., 2001. Biomass accumulation and main stem elongation of durum wheat grown under mediterranean conditions. Ann. Bot. 88, 617–627. https://doi.org/10.1006/anbo.2001.1512.

Viña, A., Gitelson, A.A., Nguy-Robertson, A.L., Peng, Y., 2011. Comparison of different vegetation indices for the remote assessment of green leaf area index of crops. Remote Sens. Environ. 115, 3468–3478. https://doi.org/10.1016/j.rse.2011.08.010.

Vincini, M., Frazzi, E., D'Alessio, P., 2008. A broad-band leaf chlorophyll vegetation index at the canopy scale. Precis. Agric. 9, 303–319. https://doi.org/10.1007/s11119-008-9075-z.

Wang, L., Zhou, X., Zhu, X., Dong, Z., Guo, W., 2016. Estimation of biomass in wheat using random forest regression algorithm and remote sensing data. Crop J. 4, 212–219. https://doi.org/10.1016/j.cj.2016.01.008.

Weiss, M., Baret, F., 2016. S2ToolBox Level 2 products: LAI, FAPAR, FCOVER - Version 1.1. Sentin. ToolBox Level2 Prod. 53.

Weiss, M., Baret, F., Myneni, R.B., Pragnère, A., Knyazikhin, Y., 2000. Investigation of a model inversion technique to estimate canopy biophysical variables from spectral and directional reflectance data. Agronomie 20, 3–22. https://doi.org/10.1051/agro:2000105.

Weiss, M., Jacob, F., Duveiller, G., 2020. Remote sensing for agricultural applications: a meta-review. Remote Sens. Environ. 236, 111402 https://doi.org/10.1016/j.rse.2019.111402.

Wolanin, A., Camps-Valls, G., Gómez-Chova, L., Mateo-García, G., van der Tol, C., Zhang, Y., Guanter, L., 2019. Estimating crop primary productivity with Sentinel-2 and Landsat 8 using machine learning methods trained with radiative transfer simulations. Remote Sens. Environ. 225, 441–457. https://doi.org/10.1016/j.rse.2019.03.002.

Woodruff, D.L., Reiners, T., 2004. Experiments with, and on, algorithms for maximum likelihood clustering. Comput. Stat. Data Anal. 47, 237–253. https://doi.org/10.1016/j.csda.2003.11.002.

Zadoks, J., Chang, T., Konzak, C., 1974. A decimal code for the growth stages of cereals. Weed Res. 14, 415–421. https://doi.org/10.1111/j.1365-3180.1974.tb01084.x.

Zhang, L., Traore, S., Ge, J., Li, Y., Wang, S., Zhu, G., Cui, Y., Fipps, G., 2019. Using boosted tree regression and artificial neural networks to forecast upland rice yield under climate change in Sahel. Comput. Electron. Agric. 166, 105031 https://doi.org/10.1016/j.compag.2019.105031.

Zhou, X., Kono, Y., Win, A., Matsui, T., Tanaka, T.S.T., 2020a. Predicting within-field variability in grain yield and protein content of winter wheat using UAV-based multispectral imagery and machine learning approaches. Plant Prod. Sci. 00, 1–15. https://doi.org/10.1080/1343943X.2020.1819165.

Zhou, X., Wang, P., Tansey, K., Zhang, S., Li, H., Tian, H., 2020b. Reconstruction of time series leaf area index for improving wheat yield estimates at field scales by fusion of Sentinel-2, -3 and MODIS imagery. Comput. Electron. Agric. 177, 105692 https://doi.org/10.1016/j.compag.2020.105692.

Zhou, X., Zheng, H.B., Xu, X.Q., He, J.Y., Ge, X.K., Yao, X., Cheng, T., Zhu, Y., Cao, W.X., Tian, Y.C., 2017. Predicting grain yield in rice using multi-temporal vegetation indices from UAV-based multispectral and digital imagery. ISPRS J. Photogramm. Remote Sens. 130, 246–255. https://doi.org/10.1016/j.isprsjprs.2017.05.003.